# Imprint of eutrophication on methane-cycling microbes in freshwater sediment

Alice Bosco-Santos[1*], Eulalie Rose Beyala Bekono[1], Santona Khatun[1,2], Marie-Ève Monchamp[3], Joana Séneca[4,5], Petra Pjevac[4,5], Jasmine S. Berg[1]

[1]Institute of Earth Surface Dynamics (IDYST), University of Lausanne, Lausanne, Switzerland

[2] School of Architecture, Civil and Environmental Engineering, Environmental Engineering Institute, Smart Environmental Sensing in Extreme Environments (SENSE), École Polytechnique Fédérale de Lausanne (EPFL Valais Wallis), 1951 Sion, Switzerland

[3]Biology Department, McGill University, Montreal, Canada

[4]Division of Microbial Ecology, Centre for Microbiology and Environmental Systems Science, University of Vienna, Vienna, Austria

[5]Joint Microbiome Facility of the Medical University of Vienna and the University of Vienna, Vienna, Austria

*(alice.boscosantos@unil.ch)

**Abstract.** Eutrophication can alter methane ($CH_4$) cycling in lakes, yet its long-term effect on sediment microbial communities remains unclear. We analyzed a 400-year-old sediment record from the historically eutrophied Lake Joux, Switzerland, combining porewater and solid-phase geochemistry with 16S rRNA gene amplicon analyses to elucidate the effects of nutrient and carbon loading on methanogenic and methanotrophic sediment communities. Lithological and chemical stratification defined three intervals (deep eutrophic, middle carbonate, upper eutrophic) correlated with changes in organic matter sources. Methanogens were clearly depth-partitioned: methylotrophic Methanomassiliicoccales dominated deep eutrophic sediments, whereas hydrogenotrophic Methanomicrobiales and Methanobacteriales increased upward in shallower, more recent sediments with fresher organic matter. Paired isotopic data support this substrate-driven shift in $CH_4$ production. Although $O_2$ was not detected below ~0.4 cm, sequences of aerobic gammaproteobacterial methanotrophs (*Crenothrix* and *Methylobacter*) were abundant in surface sediments down to ~20 cm sediment depth, correlating with $NO_3^-$ and $PO_4^{3-}$ concentrations. The absence of anaerobic methanotrophs and C-isotopic evidence for ongoing methane oxidation suggest that these $O_2$-requiring, methane monooxygenase-utilizing Methylococcales constitute the dominant $CH_4$ sink in surface sediments. These findings reveal that eutrophication can cause a stratification of methane-cycling microbial communities, highlighting the role of sedimentary legacies in regulating benthic $CH_4$ emissions from freshwater ecosystems.

## 1. Introduction

Freshwater ecosystems are significant sources of the greenhouse gas methane ($CH_4$), with natural lakes estimated to contribute more than 70% to freshwater $CH_4$ emissions (Sanches et al., 2019). Despite their substantial contribution to atmospheric $CH_4$, the mechanisms regulating $CH_4$ emissions from lakes at regional and global scales remain poorly understood (Bastviken et al., 2011; Sanches et al., 2019). In freshwater sediments, $CH_4$ is abundantly produced via anaerobic methanogenesis by archaea (Bastviken et al., 2004; Bastviken et al., 2011; Conrad, 2020; Dean et al., 2018; Saunois et al., 2020; Tranvik et al., 2009). Methanogens can respire different substrates produced during organic matter remineralization and are classified according to three known pathways for $CH_4$ production: hydrogenotrophic (carbon dioxide reduction using hydrogen), acetoclastic (splitting acetate), and methylotrophic (using methylated compounds like methanol) (Garcia et al., 2000). Environmental factors such as substrate concentration, temperature, salinity, and pH influence the predominance of these pathways, with methylotrophic methanogenesis, for instance, being favored at higher salinity and acidity (Bueno De Mesquita et al., 2023; Yvon-Durocher et al., 2014).

Much of the $CH_4$ produced in lake sediments is oxidized through both aerobic and anaerobic microbial processes before it can reach the atmosphere (Bastviken et al., 2004; Bastviken et al., 2008; Martinez-Cruz et al., 2017; Martinez-Cruz et al., 2018; Oswald et al., 2016). Aerobic oxidation, predominantly performed by methane-oxidizing bacteria (MOB) from the Gammaproteobacteria and Alphaproteobacteria classes, occurs at the sediment-water interface and in the water column (Hanson and Hanson, 1996; Knief, 2015). All MOB known to date rely on $O_2$-dependent methane monooxygenase enzymes and oxidize up to 90% of sediment-derived $CH_4$, thus helping to mitigate greenhouse gas emissions from freshwater ecosystems (Bastviken et al., 2004; Bastviken et al., 2008). Anaerobic oxidation of methane (AOM) is performed by methanotrophic archaea (ANMEs), often in partnership with bacteria that use electron acceptors other than oxygen (Knittel and Boetius, 2009; Milucka et al., 2012; Wegener et al., 2015). In marine environments where sulfate concentrations are high, sulfate-AOM is the dominant process (Jørgensen et al., 2001; Wegener and Boetius, 2009). In contrast, the electron acceptors sulfate, nitrate/nitrite, humic substances, and diverse metal oxides contribute in various degrees to AOM in freshwater sediments (Chen et al., 2023; Deutzmann and Schink, 2011; Martinez-Cruz et al., 2018; Zhao et al., 2024).

Recently, it has been proposed that eutrophication induced by anthropogenic nutrient inputs (e.g., nitrates and phosphates) into lake ecosystems influences methanogen and methanotroph community structure by altering organic matter quality and quantity (Beaulieu

et al., 2019; Yang et al., 2021; Yang et al., 2019; Yang et al., 2020; Zhu et al., 2022). The influx of organic carbon from phytoplankton blooms enhances organic matter mineralization in lake bottom waters and sediments, depleting electron acceptors such as oxygen ($O_2$), nitrate ($NO_3^-$), sulfate ($SO_4^{2-}$), and metal oxides (Fe(III), Mn(IV)). The decomposition of phytoplankton biomass also releases significant amounts of methyl-sulfur compounds, favoring methylotrophic $CH_4$ production (Penger et al., 2012; Tebbe et al., 2023; Tsola et al., 2021; Yan et al., 2017; Zhou et al., 2022). Anaerobic conditions, combined with increased organic matter availability, are expected to boost methanogenesis, resulting in elevated $CH_4$ release following eutrophication (Fiskal et al., 2019; Sanches et al., 2019; Zhou et al., 2022).

Conversely, nutrient addition can stimulate microbial $CH_4$ oxidation (Yang et al., 2019). Some aerobic MOB can oxidize $CH_4$ while respiring $NO_3^-$ (denitrification), and a growing body of evidence supports the widespread occurrence and activity of these bacteria in $O_2$-limited environments (Almog et al., 2024; Kits et al., 2015; Reis et al., 2024; Schorn et al., 2024). Importantly, MOB exhibit niche partitioning along $O_2$–$CH_4$ and nutrients gradients with Gammaproteobacteria, Alphaproteobacteria, and nitrite-dependent taxa that produce $O_2$ intracellularly, such as *Candidatus Methylomirabilis,* occupying distinct layers (Mayr et al., 2020; Reis et al., 2020). Gammaproteobacterial MOB are generally associated with fast-growing life strategies in resource-rich conditions, whereas alphaproteobacterial MOB are adapted to resource-limited or stable environments (Ho et al., 2013). Indeed, P and N enrichment, for instance, can increase $CH_4$ oxidation rates and favor Gammaproteobacterial over Alphaproteobacterial MOB (Nijman et al., 2022; Veraart et al., 2015). Together, these findings highlight that nutrients modulate both $CH_4$ production and consumption, adding complexity to how eutrophication shapes lacustrine $CH_4$ dynamics (Nijman et al., 2022; Reis et al., 2020; Veraart et al., 2015; Wei et al., 2022).

Eutrophication of lakes in Switzerland reached critical levels during the mid-20$^{th}$ century, particularly in the 1950-1970s, due to rapid industrialization, urbanization, and agricultural intensification. Public outcry and scientific research prompted the introduction of wastewater treatment plants and stricter regulations on phosphate detergents, leading to significant improvements in water quality by the late 20$^{th}$ century. Nevertheless, sediments retain a legacy of this eutrophication in the form of increased organic matter content (Fiskal et al., 2019), which continues to shape microbial community structure (Han, 2020) long after lake waters recovered. Some studies have reported clear vertical zonation of methanogenic and methanotrophic communities in relation to trophic history and electron acceptor distributions (Rissanen et al., 2023; Van Grinsven et al., 2022), while others found little to no stratification

(Meier et al., 2024). Consequently, the cascading impacts of anthropogenic nutrient inputs on the balance of $CH_4$ production and oxidation in lake sediments remain poorly constrained.

Here, we test whether historical eutrophication has left a sedimentary legacy that structures contemporary methane-cycling communities in Lake Joux (Vaud, Switzerland), a site with a well-documented history of trophic regime shifts and phytoplankton bloom deposits (Lavrieux et al., 2017; Monchamp et al., 2021). Using a ~400-year, 55-cm sediment archive, we combine porewater and solid-phase geochemistry, 16S rRNA gene amplicon profiling, and stable-carbon-isotope measurements to resolve depth zonation of methanogens and methanotrophs, and link community shifts to organic-matter sources, lithology, and redox conditions. By explicitly coupling the depositional record to present microbial community structure and isotope compositions of different carbon pools, we provide process-level constraints relevant for forecasting benthic $CH_4$ in eutrophying and recovering lakes.

## 2. Materials and methods

### *2.1* Study Area

Lake Joux is a perialpine lake in the Joux Valley in the Swiss Jura Mountains (Fig. 1A). The valley developed in a Jura syncline, marked by glacial erosion and Quaternary deposits, and it lies mainly on Upper Jurassic and Tertiary limestones. The lake has an average depth of 32 m, a surface area of approximately 9 $km^2$ (maximum 9 km in length and 1 km in width), and a watershed covering around 211 $km^2$. Situated at an altitude of 1,183 meters, the lake is subject to intense seasonal variations and meteorological events, which drive the runoff of both natural and anthropogenic materials.

Human activity in the watershed dates back over 6,850 years (Lavrieux et al., 2017; Mitchell et al., 2001; Monchamp et al., 2021). By the 16$^{th}$ century, the area around Lake Joux became more densely populated, leading to land drainage and deforestation for livestock farming (Piguet, 1946). Frequent crop failures and food shortages during the late 17$^{th}$ century spurred the growth of glassmaking and lapidary industries. Horology, introduced in the 18$^{th}$ century, became the region's dominant economic activity by the 19$^{th}$ century. This period of industrialization resulted in a transition from cultivated farmland to pastures and fallow fields (Lavrieux et al., 2017).

Agricultural intensification and urban expansion during the 20$^{th}$ century significantly increased nutrient inputs to Lake Joux, resulting in pronounced eutrophication. Phosphorus levels peaked at 35 µg/L in 1979 (Lods-Crozet et al., 2006), triggering major ecological

changes, including rapid shifts in phytoplankton communities as eutrophication-adapted taxa outcompeted the lake's original species (Monchamp et al., 2021). A re-oligotrophication phase began in 1988–1989 following improved nutrient management and mitigation efforts. However, despite these reductions in external nutrient loading, the lake has not returned to its pre-eutrophication conditions. More than 70 years after the documented episode of eutrophication, the water column remains altered, suggesting that the system has shifted to an alternative stable state with a biological configuration resistant to reversal (Lods-Crozet et al., 2006; Monchamp et al., 2021).

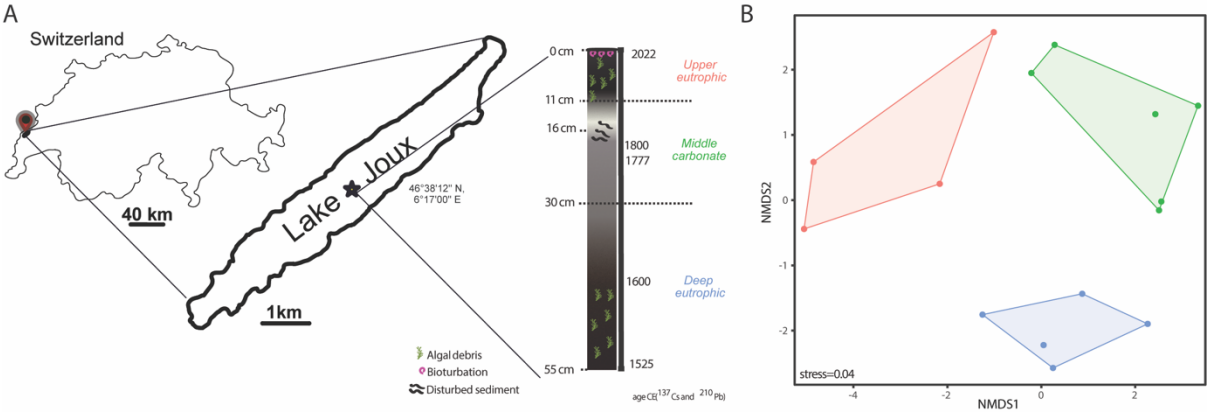


**Figure 1** – (A) Location of Lake Joux (Switzerland; sampling in 2023) and 55 cm core schematic representatio with the three stratigraphic intervals identified from lithology and age markers: deep eutrophic, middle carbonate, and upper eutrophic. **(B)** Non-metric multidimensional scaling (NMDS) of the porewater and solid-phase geochemical dataset, showing separation of samples by stratigraphic interval (upper eutrophic = red, middle carbonate = green, deep eutrophic = blue). Points are individual depth samples; colored polygons outline the convex hull for each interval and symbols mark group centroids. Ordination was performed on z-scored variables using Bray–Curtis dissimilarities.

## *2.2* Sampling

In May 2023, three gravity cores (45-55 cm long) were recovered from the lakebed of Lake Joux using a Uwitec gravity corer. The cores were taken from one of the deepest parts of the lake (46°38'12" N, 6°17'00" E; 28 m depth) and sealed with rubber caps. One core was pre-drilled and taped at 3 cm intervals to facilitate rapid $CH_4$ sampling using 3 ml syringes on shore. The other two cores, one for porewater and the other for sediment chemistry and microbiome analyses, were processed in the laboratory within 24 h. Porewater was extracted via $N_2$ flushed syringes attached to 0.2 µm Rhizons (Rhizosphere), inserted every 3 cm along the core, stored at 4°C and analyzed within 48 h. The third sediment core was opened with a

handheld saw and sectioned every 3 cm. Each solid sample was split into an acid-cleaned vial and a sterile vial, then frozen at -20°C.

### *2.3* Porewater chemistry

Porewater samples for dissolved anions ($PO_4^{3-}$, $NO_3^-$, $NO_2^-$, $SO_4^{2-}$) were transferred to plastic vials while flushing with $N_2$, capped, and analyzed using an ion chromatograph (DX-ICS-1000, DIONEX) equipped with an AS11-HC column. For dissolved inorganic carbon (DIC) porewater samples were filled into 1.5 ml borosilicate vials and capped headspace-free to prevent $CO_2$ degassing. DIC concentration (mmol $L^{-1}$) was obtained from the $CO_2$ yield after acid conversion of aliquots transferred to helium-flushed Exetainers containing 200 µL of 99% $H_3PO_4$, and the resulting $CO_2$ peak areas were quantified on a GasBench II (Thermo Fisher Scientific). A response factor (µmol $CO_2$ per peak-area unit) was derived from identically processed Carrara Marble (CM) standards and applied to the second $CO_2$ peak of each sample; moles of $CO_2$ were converted to DIC using the injected sample volume. External uncertainty on DIC concentration, based on CM reproducibility, was <7%. For $\delta^{13}C_{DIC}$, the headspace $CO_2$ was analyzed by GasBench II coupled to a Delta V Plus IRMS; each sample was measured six times, and we report the mean with 1σ (typically <0.10‰). Values were normalized to the in-house CM standard ($\delta^{13}C$ = +2.05‰) calibrated against NBS-19 and NBS-18; external reproducibility from CM replicates (n = 12) was <0.05‰ (1σ). Carbon isotopes are reported in delta (δ) notation relative to the Vienna Pee Dee Belemnite (VPDB) standard, defined as $\delta = ((R_{sample} \backslash R_{standard}) - 1) \times 1000$ ‰, with *R* the $^{13}C/^{12}C$ ratio; positive δ indicates enrichment in $^{13}C$ relative to Vienna Pee Dee Belemnite (VPDB) standard. For dissolved sulfide analysis, porewater was fixed with 0.05 M Zn-acetate ($Zn(CH_3COO)_2 \cdot 2H_2O$) solution at a 1:2 ratio immediately after extraction, and dissolved sulfide was quantified photometrically using the methylene blue method (Cline, 1969).

### *2.4* Sediment description and chemistry

Sediment from the opened core was visually assessed (using standard charts) for color and granulometry based on observable differences in particle size, texture, and sorting within the sediment layers. Lithological boundaries in our core were aligned to the dated Lake Joux record of Lavrieux et al. (2017) using their carbonate sediment interval (whiter sediments) as reference. Ages were transferred from their $^{210}Pb/^{137}Cs$ model; uncertainties are those reported therein.

For total phosphorus (P), ~1 g of wet sediment was digested in 9 ml of 4:2 $HNO_3$:HCl using an Anton Paar microwave system, filtered (0.45 µm glass fiber), and analyzed by inductive coupled plasma-optical emission spectrometry (ICP-OES, Agilent 5800). Calibration used a multi-element standard, with certified reference materials yielding 85–102% recovery.

Elemental C, N, H, and S were measured on 1–3 mg of freeze-dried sediment using a UNICUBE (Elementar®) at EPFL's ISIC-MSEAP. Total organic carbon (TOC) and total inorganic carbon (TIC) were estimated by loss on ignition (500°C and 1200°C). $\delta^{13}C_{org}$ was determined by Elemental Analyzer–Isotope Ratio Mass Spectrometry (EA-Isolink IRMS, Thermo Fisher) after 48 h treatment with 6 N HCl to remove carbonates. Results are reported in delta notation related to VPDB, as described above for $\delta^{13}C_{DIC}$), with a reproducibility better than 0.2‰.

Acid-volatile sulfur (AVS) and chromium-reducible sulfur (CRS) were extracted from 1–2 g of frozen sediment as per Spangenberg and Bosco-Santos (2024). Sulfide in AVS and CRS fractions was measured colorimetrically (Cline, 1969) and CRS sulfur isotopic composition ($\delta^{34}S_{crs}$) by IRMS (Spangenberg and Bosco-Santos, 2024). These measurements help distinguish easily mobilized sulfide pools (AVS) from more stable sulfur forms (CRS) in sediments.

### *2.5* Dissolved oxygen and methane

Oxygen concentrations were measured using a 200 µm-tip glass microsensor (Unisense) after 2-point calibration in Na-dithionite and air-saturated water. Seven vertical profiles from the same core were recorded at 250 µm steps with a motorized controller and Field Multimeter (Unisense).

For $CH_4$ analysis, 3 $cm^3$ of sediment was transferred into 100 ml serum bottles with 5 ml of 10% NaOH, sealed, and homogenized. Dissolved $CH_4$ was extracted by headspace displacement and quantified via gas chromatography (Joint Analytical Systems) equipped with an FID at the Eawag (Khatun et al., 2024). $\delta^{13}C_{CH4}$ was measured using Gas Chromatography–Combustion–Isotope Ratio Mass Spectrometry (GCC-IRMS,Agilent 6890N with Thermo Finnigan IRMS) and analyzed with IonVantage software (Khatun et al., 2024). Results are reported in delta notation relative to VPDB with an analytical error <1.1‰.

Carbon isotopic fractionation factors (α) between organic carbon ($\delta^{13}C_{org}$ ,substrate) and methane ($\delta^{13}C_{CH4}$,product were calculated as: $\alpha = (\delta^{13}C_{org} + 1000)/(\delta^{13}C_{CH4} + 1000)$). The

corresponding isotopic fractionation (ε, ‰) was then determined by the relationship $\varepsilon = (\alpha - 1) \times 1000$, allowing interpretation of trends in dominant methanogenic pathways.

In order to determine sediment zonation by environmental variables, we performed non-metric multidimensional scaling (NMDS) on a Euclidean distance matrix of z-scored environmental data for samples between 0.5 and 43.5 cm sediment depth, using the function metaMDS() in the R package vegan. The NMDS stress value was 0.04. Differences among depth-defined clusters based on environmental variables were tested using a permutational multivariate analysis of variance (PERMANOVA) on smoothed Euclidean distance matrices.

### *2.6* DNA extraction and 16S rRNA gene amplicon analysis

DNA was extracted from Lake Joux sediments using the PowerSoil Pro Kit (Qiagen). Extraction, sequencing, and raw data processing were conducted at the Joint Microbiome Facility (Medical University of Vienna and University of Vienna; project ID JMF-2310-14). The V4 hypervariable region of the 16S rRNA gene was amplified and sequenced to assess the total microbial diversity in the collected samples. Amplification was performed with linker-modified 515F and 806R (Apprill et al., 2015; Parada et al., 2016) primers, and amplicons were barcoded, multiplexed, sequenced on an Illumina MiSeq (v3 chemistry, 2x 300 bp), and extracted from the raw sequencing data as described in detail in Pjevac et al. (2021). Amplicon Sequence Variants (ASVs) were inferred using the DADA2 R package v1.42 (Callahan et al., 2016b), applying the recommended workflow (Callahan et al., 2016a). FASTQ reads 1 and 2 were trimmed at 220 nt and 150 nt with allowed expected errors of 2. ASV sequences were subsequently classified using DADA2 and the SILVA database SSU Ref NR 99 release 138.1 (Quast et al., 2012; Mclaren and Callahan, 2021) using a confidence threshold of 0.5. ASVs without classification or classified as eukaryotes, mitochondria, or chloroplasts, as well as well-known buffer contaminations, were removed. After filtering, only samples with at least 7000 read pairs were kept for further analyses, and relative abundances of ASVs grouped at higher taxonomic levels were calculated in relation to all remaining data**.** The relative abundance of chloroplast sequences, which were removed from the microbial community dataset, was examined separately to assess phytoplankton debris abundance across the sediment profile.

Downstream analyses were performed using R v4.3.2 and Bioconductor v3.16 packages SummarizedExperiment v1.32, SingleCellExperiment v1.24, TreeSummarizedExperiment v2.8 (Huang et al., 2021), mia v1.8 (https://github.com/microbiome/mia), LMdist (Hoops and Knights, 2023), vegan 2.6-8,

phyloseq v1.44 (Mcmurdie and Holmes, 2013) (Vegan R package; phyloseq R package), microbiome v1.22 (http://microbiome.github.io), microViz v0.10.8 (Barnett et al., 2021), and corrplot (Wei, 2024). Microbial community alpha diversity indices were calculated on rarified 16S rRNA gene amplicon data using R packages vegan and mia. For community dissimilarity analysis, microbial 16S rRNA gene amplicon sequence count data was centered log ratio (CLR) transformed, a pairwise Aitchison distances matrix was computed, and oversaturated distances in the dissimilarity matrix were corrected and smoothed using LMdist with default settings prior to ordination using principal coordinates analysis (PCoA). Differences in 16S rRNA gene amplicon community composition among three depth-defined clusters were tested using permutational multivariate analysis of variance (PERMANOVA) on an Aitchison distance-based dissimilarity matrix.

To identify the environmental variables that significantly contributed to the variation in microbial community structure, correlations between microbial community composition and environmental variables were assessed using Mantel tests, based on Euclidean distances calculated from Z-score standardized environmental variables and LMdist corrected and smoothed Aitchison distances of 16S rRNA gene amplicon sequencing data. Prior to correlation analysis, five samples from the deep eutrophic layer without corresponding environmental data were excluded. Mantel tests were performed using Spearman's rank correlation as implemented in the R package vegan. The resulting p-values were adjusted for multiple testing using the false discovery rate (FDR) method. Highly correlated environmental variables (Spearman's r>0.8, Figure S1), as assessed by the function cor() in the R package corrplot, were removed before the Mantel tests.

## 3. Results

### *3.1* Sediment description

The 55-cm deep sediment record of Lake Joux could be classified into three main intervals based on distinct lithological and chemical features (Fig. 1 and Supplementary Fig. 1). The 'deep eutrophic' interval, from 55 cm to 30 cm, comprises black and silty sediments, indicating a period of higher lake productivity and low oxygen conditions. Occasional fine sand and organic fibers are also present. In the 'middle carbonate' interval, from 30 cm to 11 cm, the sediments transition from a murky gray with heterogeneous brownish features, suggesting changes in organic matter quality and oxidation states (Fig. 1) to whitish silty-sandy sediments, with the contribution of shells above 13.5 cm, indicating the dominant deposition of carbonates

(Fig. 1). The 'upper eutrophic' interval, from 11 cm to 0 cm, contains intensely black sediment with frequent plant debris, reflecting recent environmental changes.

To assign approximate ages to our sedimentary profile, we correlated our lithological intervals to other Lake Joux sedimentary sequences previously published and dated using $^{237}Cs$ and $^{210}Pb$ (Lavrieux et al., 2017; Magny et al., 2008) (Fig. 1). The middle carbonate unit (30–11 cm) in our core aligns with their U3–U4 carbonate interval, including the distinctive pale "white" boundary at ~16–11 cm. The overlying upper eutrophic black, organic-rich sediments (11–0 cm) correspond to U5, which spans the 20th-century eutrophication phase and includes the $^{137}Cs$ markers at ~1954 and ~1963 in the Lavrieux record. By transfer of their age–depth model, the base of our deep eutrophic interval (below 30 cm) falls in the late 16th–early 17th century. Reported sedimentation rates in Lavrieux (≈0.04–0.11 cm $yr^{-1}$ before the 18th century, a short-lived peak ≈0.83 cm $yr^{-1}$ in the late 18th century, and ≈0.18 cm $yr^{-1}$ over recent decades) are consistent with the thicknesses of our corresponding units (Lavrieux et al., 2017).

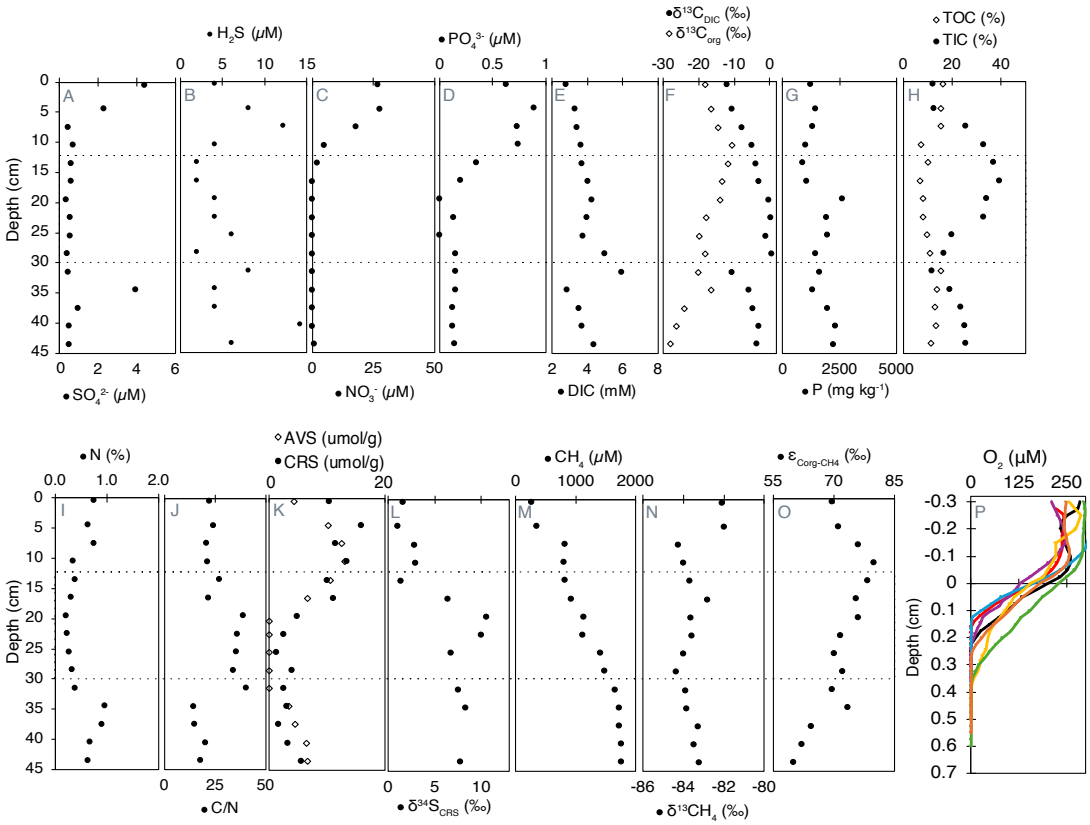


**Figure 2** - Geochemical profiles of porewater, solid-phase compounds, and dissolved gases in Lake Joux sediments. Dashed lines represent the transitions between the *'deep eutrophic'* interval from 55 to 30.5 cm, the *'middle carbonate'* interval from 28.5 to 11 cm, and the *'upper eutrophic'* from 11 to 0 cm. All data are available in Table S1 (panels A to N) and Table S2 (panel O).

348

349 ### *3.2* Porewater chemistry

350 Sulfate ($SO_4^{2-}$, between 0.35 μM and 4.5 μM) and dissolved sulfide ($H_2S$, between 2 μM
351 and 14.3 μM) were measurable throughout the entire sedimentary profile. In the upper
352 eutrophic interval (0 – 11 cm), opposing gradients of $SO_4^{2-}$ and $H_2S$ from the surface to 7.5
353 cm are evidence of sulfate reduction (Fig. 2A, B). Below this depth, sulfate is absent, but a
354 broad $H_2S$ maximum in the deep eutrophic sediments (~40 cm) could be associated with
355 organic sulfur degradation.

356 Dissolved nitrate ($NO_3^-$) and phosphate ($PO_4^{3-}$) first appeared at 19.5 cm and 16.5 cm,
357 respectively, with concentrations progressively increasing toward the surface, reaching
358 maximum values of 27 μM for $NO_3^-$ and 0.62 μM for $PO_4^{3-}$ (Fig. 2C and 2D). Nitrite
359 concentrations were close to the detection limit (0.03 μM) and uniformly low (range 0.038–
360 0.087 μM, median ≈0.043 μM) with no systematic depth trend (Fig. S2).

361 Dissolved inorganic carbon (DIC) concentrations with isotopically heavier composition
362 ($\delta^{13}C_{DIC}$) were highest in the middle carbonate interval between 16.5 cm and 31.5 cm (Fig. 2E
363 and F). Above 7.5 cm depth, $\delta^{13}C_{DIC}$ values became progressively lighter toward the surface,
364 reaching a minimum of -12‰ (Fig. 2F).

365

366 ### *3.3* Sediment chemistry

367 #### 3.3.1 Phosphorous and organic matter characterization

368 Total phosphorus (P) content, ranging from 860 to 2612 mg $kg^{-1}$, was generally higher
369 in the deeper sediments and progressively decreased towards the surface, except for a sharp
370 peak at 19.5 cm depth (Fig. 2G). Organic carbon (TOC) exhibited higher concentrations in both
371 the deep eutrophic and upper eutrophic sediments, contrasting with TIC content, which peaked
372 in the middle carbonate interval (Fig. 2H). The $\delta^{13}C_{org}$ was lightest in the deep eutrophic
373 sediments (-28.22‰ at 43.5 cm) and heaviest in the upper eutrophic sediments (-10.76‰ at
374 10.5 cm) (Fig. 2F).

375 Nitrogen content followed the same pattern as TOC, with higher N in the deep and
376 upper eutrophic sediments compared to the middle carbonate region (Fig. 2I). The ratio
377 between C and N, a qualitative parameter of organic matter source (Meyers, 1994), exhibited
378 relatively lower values in the deep eutrophic sediments, increasing in the middle carbonate
379 sediments and decreasing again in the upper eutrophic sediments (Fig. 2J).

380

### 3.3.2 Solid-phase sulfides

Acid volatile sulfides (AVS) were measurable in the deep eutrophic sediments between 43.5 and 34.5 cm and within the upper eutrophic sediments above 19.5 cm depth. The maximum concentrations of AVS in the upper eutrophic sediments (around 418 μg $kg^{-1}$ at 10.5 cm) were about twice as high as in deep eutrophic sediments (200 μg $kg^{-1}$ at 40.5 cm) (Fig. 2K). Chromium reducible sulfur (CRS) also exhibited higher concentrations in the shallower sediments, becoming more prominent from 16.5 cm depth to the surface. CRS concentrations were more variable than AVS, varying from 23 μg $kg^{-1}$ to 510 μg $kg^{-1}$ (Fig. 2K). The isotopic composition $\delta^{34}S$ of CRS was positive throughout the profile, ranging from ~1‰ near the surface to a maximum of 10.5‰ at 19.5 cm depth. Values remained elevated in the middle carbonate and deep eutrophic zones (e.g., 8.3‰ at 34.5 cm and 7.7‰ at 43.5 cm), indicating that the reduced sulfur pool is isotopically enriched in $^{34}S$ across the sediment column (Fig. 2L).

### 3.3.3 Dissolved oxygen and methane

Methane ($CH_4$) concentrations were highest in the deep eutrophic sediments, with a maximum of approximately 1760 μM at 45 cm depth. From 31.5 cm depth, $CH_4$ exhibited a clear decreasing trend, reaching the lowest concentration (253 μM) at the surface (Fig. 2M). The most significant drop in $CH_4$ concentrations occurred between 7.5 and 4.5 cm depth, where the concentrations decreased by half (Fig. 2M). The $\delta^{13}C_{CH_4}$ exhibited minimal variation along the profile, averaging -83.0 ± 0.7‰. The most pronounced isotopic shift (>2.2‰) towards heavier values occurred at the same depth as the sharp decline in $CH_4$ concentration (Fig. 2N).

Fractionation factors (α) between $C_{org}$ and $CH_4$ ranged from 1.069 to 1.080 across sediment depths, corresponding to carbon isotope fractionations (ε) of 69‰ to 80‰ (Fig. 2O). These values reflect the measurable discrimination between $^{13}C$ and $^{12}C$ during $CH_4$ production from organic substrates, which arises from the enzymatic pathways and substrates utilized. Lower ε values were consistently observed in deeper sediments compared to shallower layers.

Oxygen concentrations were measured across seven different profiles, and free $O_2$ was detectable only in the uppermost sediments, between 0.165 cm and 0.365 cm depth (Fig. 2P). Below 0.4 cm, sediments were consistently anoxic. The heterogeneous penetration of $O_2$ into the sediments is attributed to bioturbation, which was confirmed by visual observations of worm castings.

### 3.3.4 Microbial community composition and chloroplast relative sequence abundances

The microbial community in Lake Joux sediments was dominated by the phyla Chloroflexota, Nanoarchaeota, and Pseudomonadota (Fig. 3A). In the upper eutrophic sediments (below 30 cm), microbial species richness and evenness (Chao1 and Shannon alpha diversity indices) were significantly lower than in overlying layers (Fig. 3C). In this zone, Nanoarchaeota reached their highest relative sequence abundances (>10%), decreasing to ~7% in the shallower sediments. These elevated abundances, also reported in freshwater (Chen et al., 2023; Xie et al., 2024) and marine environments (Brick et al., 2025), likely reflect their wide environmental tolerance and host associations (Jarett et al., 2018) (Fig. 3A).

In the middle carbonate-rich interval (30–11 cm), microbial diversity increased, and Bacteroidota appeared, consistently representing >5% of the microbial community. Reduced relative abundances of chloroplast sequences in this layer (Fig. 3B) also indicate limited input from photosynthetic organisms during this depositional phase. Cyanobacteria-related ASVs displayed similar depth trends to chloroplast sequences, but with lower overall abundance, reaching a maximum of 2% at 4.5 cm depth (Fig. 3B). In the upper eutrophic sediments (11–0 cm), Pseudomonadota became more abundant (>20%) and chloroplast sequences markedly increased, reflecting enhanced sedimentation of photosynthetic organisms.

Microbial community composition was more similar within sedimentary intervals than between them (Fig. 3D). The separation of samples into three depth clusters based on sediment biogeochemistry was statistically supported (PERMANOVA: $F = 25.05$, $R^2 = 0.81$, $p < 0.001$, Figure 3D). Significant differences in microbial community composition between the three depth clusters were also observed (PERMANOVA: methanogens - $F = 10.57$, $R^2 = 0.64$, $p < 0.001$; MOB - $F = 13.32$, $R^2 = 0.69$, $p < 0.001$; Cyanobacteria - $F = 6.57$, $R^2 = 0.52$, $p < 0.001$; Chloroplasts - $F = 8.4$, $R^2 = 0.58$, $p < 0.001$; Fig. S4). Stratification was especially pronounced for cyanobacterial and chloroplast sequences, which formed three distinct depth-specific clusters corresponding to the eutrophic, carbonate, and deep eutrophic intervals (Fig. S4). The methanotrophic community separated into two main groups, upper and deep eutrophic, while samples from the carbonate layer did not form a distinct cluster (Fig. S4). Methanogens, however, displayed clearer depth partitioning, with methylotrophic Methanomassiliicoccales dominating in the deep eutrophic interval and hydrogenotrophic Methanobacteriales increasing toward the surface (Fig. 4). Notably, depth patterns in methanogens and methanotrophs, as well as cyanobacterial and chloroplast-related sequences, tracked the same environmental gradients,

with $CH_4$, $NO_3^-$, and CRS showing the strongest correlations and AVS, $\delta^{13}C_{org}$, and sedimentary P exhibiting secondary correlations (Fig. 3E; Fig. S3).

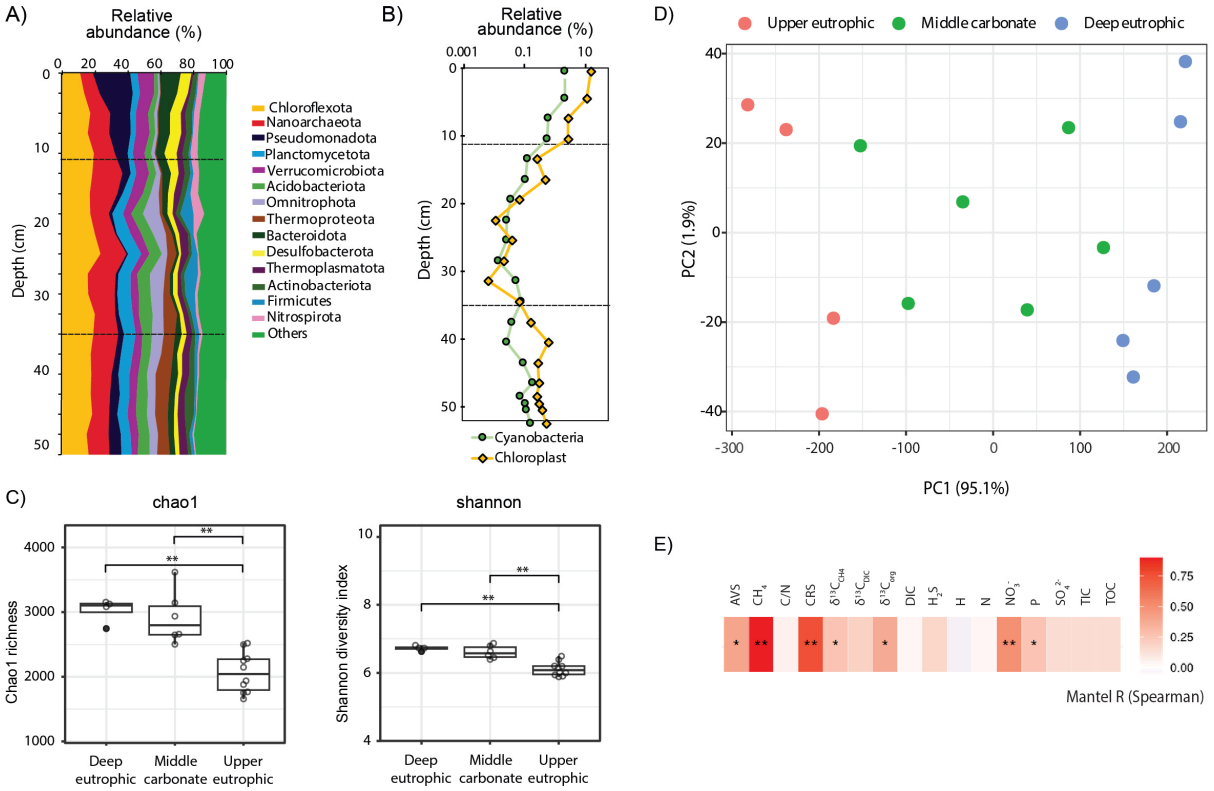


**Figure 3 -** (A) Relative 16S rRNA gene amplicon sequence abundances of bacterial and archaeal phyla, depicted as depth distribution in the 55 cm sedimentary profile of Lake Joux distribution; (B) Relative abundance of cyanobacteria and chloroplasts (algae and plants) affiliated 16S rRNA gene amplicon sequences in the 55 cm sedimentary profile of Lake Joux; (C) Alpha diversity (chao1 richness and Shannon diversity) of methanogens and methanotrophs. (D) Principal component ordination of centered log ratio (CLR) transformed 16S rRNA gene amplicon data, based on an Aitchison distance for which oversaturated distances were corrected and smoothed using LMdist. (E) Mantel tests results (Spearman's rank correlation) of community dissimilarity (corrected and smoothed Aitchison distance) and environmental parameters (z-scored). P-values were adjusted for multiple testing using the false discovery rate (FDR) method. ** p <= 0.01; * p <= 0.05.

### 3.3.4.1 Methanogenic and methanotrophic microbial communities

The relative sequence abundance of methanogens consistently accounted for more than 1% of the microbial community across all sampled depths (Fig. 4A). Methanomassiliicoccales, which are $H_2$ dependent methylotrophs, were the dominant methanogenic group in the deep eutrophic sediments, accounting for 1.4% of the microbial community at a depth of 37.5 cm (Fig. 4A). In contrast, Methanomicrobiales (hydrogenotrophs) was the most abundant methanogen group in the middle carbonate interval, (reaching 2.1% of the microbial

community) while Methanobacteriales (hydrogenotrophs) sequences were most abundant in the upper eutrophic sediments (11–0 cm, reaching 1.18% of the microbial community, Fig. 4A). Sequences affiliated with Methanosarciniales (metabolic versatile) were rare throughout the profile (<0.01%).

Across samples, the relative sequence abundances of *Crenothrix* and *Methylobacter* showed significant positive correlations with porewater $PO_4^{3-}$ and $NO_3^-$ (Spearman, $\boldsymbol{p} < 0.05$; Fig. 5). By contrast, methanogen families tracked depth-defined intervals rather than these nutrients (Fig. 4). In the deep and middle sediments below 19.5 cm, Rhizobiales-affiliated methylotrophs (e.g., Methylocystis, Methylocapsa, Methyloligellaceae) (Tamas et al., 2014; Vekeman et al., 2016) were the dominant putative methanotrophs, although they represented a modest portion of the community (max. 0.6%) (Fig. 4B). Anaerobic methanotrophs from ANME archaeal groups could not be identified in the sedimentary profile of Lake Joux. Still, between 23 and 16 cm, Methylomirabilota NC10 bacteria capable of nitrite-dependent methane oxidation with intracellularly produced $O_2$ under anoxic conditions (Ettwig et al., 2010) were detected at a relative abundance of 0.2–1.3%.

The 16S rRNA gene sequences of aerobic MOBs represented between 0.3% and 8.7% of the microbial community throughout the sediment profile and were especially numerous (>1%) above a depth of 19.5 cm (Fig. 3C). The most abundant methanotrophs from 19.5 cm depth to the surface were members of the order Methylococcales, with two genera prevalent near the surface: *Crenothrix* and *Methylobacter* (Fig. 4B). At the resolution available with V4-region 16S rRNA gene amplicon analyses, limited within-group diversity is detected, as 4 ASVs affiliated with *Methylobacter*, 17 ASVs with *Crenothrix*, and a small number of ASVs assigned to other Methylococcales genera, including a single abundant *Methylomonas* ASV (Figure S1), were recovered. Within the MOB community, the fraction of the *Methylomonas* ASV increased with depth (≈30% to ≈70%). By contrast, the fraction of the three most abundant *Crenothrix* ASVs within the MOB was stable across depth. The abundance of all individual MOB ASVs decreased with depth, relative to the total community (Figure S1).

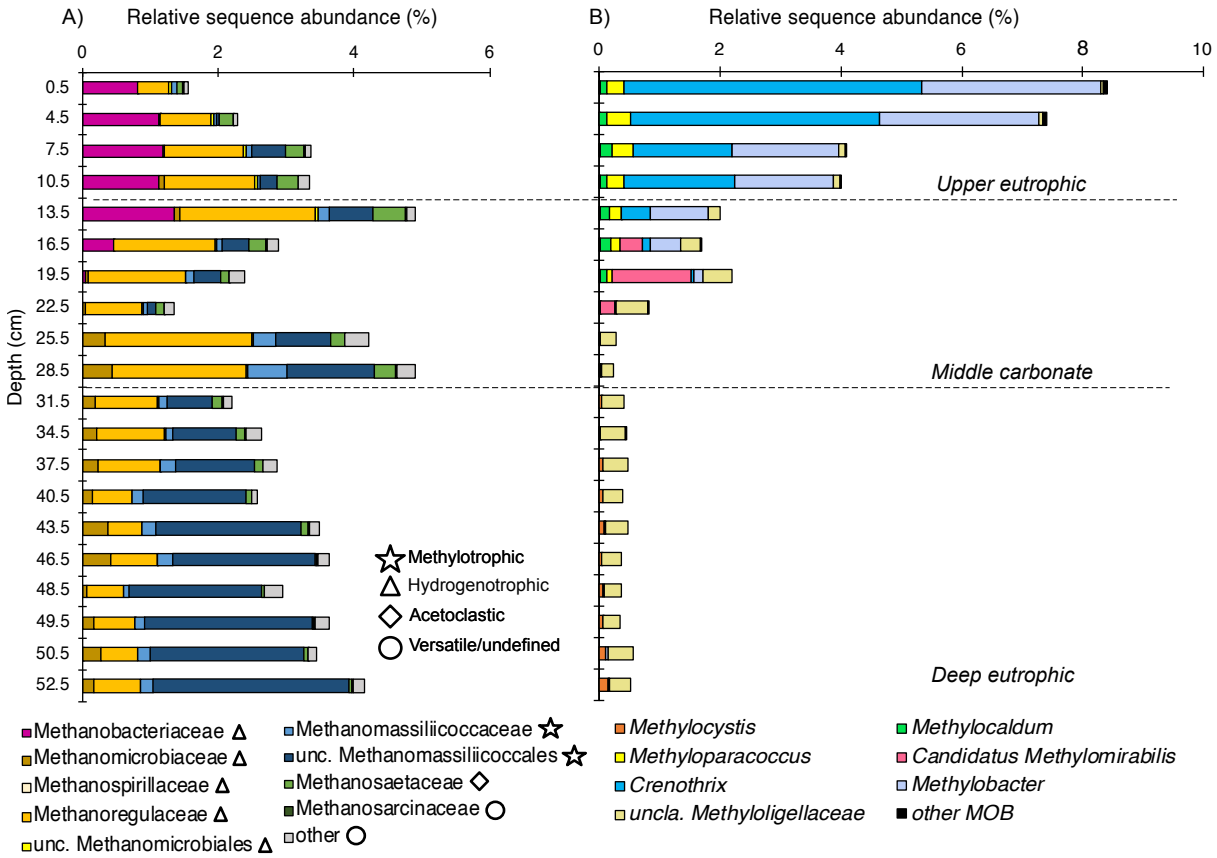


**Figure 4.** Depth-resolved composition of methanotrophic and methanogenic taxa in Lake Joux sediments. **(A)** Methanogenic archaea clustered by family/order (relative sequence abundance of total community), and grouped by inferred pathways (methylotrophic, hydrogenotrophic, acetoclastic, versatile/undefined). **(B)** Methanotrophic bacteria, including canonical MOB and Candidatus *Methylomirabilis* (NC10), were expressed as relative sequence abundance of the total community.

## 4. Discussion

### *4.1* Tracing historical land use, industrialization, and eutrophication

The intensely black sediments abundant in chloroplast-related sequences and elevated TOC content with low C:N ratios and light $\delta^{13}C_{org}$ in the deep eutrophic interval (55–30 cm, Fig. 1) attest to a predominantly autochthonous organic matter, derived from phytoplankton blooms (Lamb et al., 2006; Morales-Williams et al., 2017). Similar patterns recorded in other Lake Joux sediment profiles (Dubois, 2016; Lavrieux et al., 2017; Magny et al., 2008) correspond to a period of intensified deforestation and settlement expansion between 1525 and 1790 CE (Dubois, 2016; Lavrieux et al., 2017; Magny et al., 2008). While no official records confirm eutrophication during this period, these anthropogenic activities likely led to increased erosion and sediment/nutrient transport, stimulating phytoplankton productivity (Fig. 1). Notably, these sediments also exhibit high relative $H_2S$ and AVS concentrations (Fig. 2B and 2K), which

518 are characteristic of late sediment diagenesis under eutrophic depositional conditions (Holmer
519 and Storkholm, 2001).
520 The middle carbonate layer (30–11 cm depth) reflects a shift towards more oligotrophic
521 conditions, likely linked to the abandonment of land-intensive activities and the switch to
522 manufacturing in the 18$^{th}$ century. In addition, the 1777 construction of a dike between Lake
523 Joux and Lake Brenet lowered the lake level by 3.6 m, mobilizing limestone-rich sediments
524 (high TIC) and terrestrial plant material with heavier $\delta^{13}C_{org}$ and higher C/N ratios (Lavrieux
525 et al., 2017; Magny et al., 2008; Monchamp et al., 2021) (Fig. 2). The sedimentological
526 transition that marks the beginning of this interval at 30 cm depth aligns with a shift from
527 methylotrophic to hydrogenotrophic methanogens (Fig. 4), likely responsible for the lighter
528 $\delta^{13}C_{DIC}$ values (Fig. 2F). Furthermore, the white-colored boundary of the middle carbonate
529 layer (16–11 cm) coincides with warmer post-Little Ice Age conditions, promoting calcium
530 carbonate precipitation and TIC enrichment (Lavrieux et al., 2017).
531 The upper eutrophic sedimentary interval (11–0 cm) consists of black sediments rich in
532 TOC, lighter $\delta^{13}C_{org}$ values, low C/N ratios, and abundant chloroplast- and cyanobacteria-
533 related sequences reflecting a well-documented 20$^{th}$ century eutrophication phase (Lavrieux et
534 al., 2017; Magny et al., 2008; Monchamp et al., 2021) (Fig. 2, Fig. 3B). Elevated nutrient levels
535 in this interval could result from external nutrient inputs trapped in porewater or from organic
536 matter remineralization. Porewaters are strongly reducing, reflected by elevated $H_2S$ and CRS,
537 and the absence of $O_2$ below 0.5 cm. Downward diffusion of $SO_4^{2-}$ meets upward-diffusing
538 $CH_4$, and in the 7.5-0 cm horizon, $CH_4$ concentrations fall sharply while $\delta^{13}C_{CH4}$ becomes
539 heavier and $\delta^{13}C_{DIC}$ lighter (Fig. 2A, B and K, M). Aerobic methanotrophy fractionates carbon,
540 preferentially consuming $^{12}CH_4$ while leaving behind heavier $CH_4$ (enriched in $^{13}C$) and can
541 produce lighter (more $^{12}C$) co-localized DIC depending and on mixing and available electron
542 acceptors. Together with the dominance of MOB and the absence of ANME-related 16S rRNA
543 gene amplicon sequences, the paired isotopic shifts observed indicate methanotrophy
544 dominated by MOB as the main $CH_4$ sink in these anoxic, nutrient-replete surface sediments.
545

546 ### *4.2* Methylotrophic methanogens selected by past eutrophication

547 Changes in organic matter sources to Lake Joux over the last four centuries appear
548 closely tied to shifts in dominant methanogenic groups within its sediments. Deep eutrophic
549 sediments, characterized by the highest $CH_4$ concentrations, are dominated by
550 Methanomassiliicoccales, which are hydrogen-dependent methylotrophic methanogens that

use $H_2$ as the electron donor and methylated one-carbon compounds (e.g., methanol, methylamines, methylated S compounds) as electron acceptors, rather than reducing $CO_2$. (Bueno De Mesquita et al., 2023; Ellenbogen et al., 2024; Söllinger and Urich, 2019; Sun et al., 2019; Wang and Lee, 1994). The decomposition of algal and cyanobacterial biomass can release methylated sulfur compounds (including DMS and dimethylsulfoxide) and methylated amines, which have stimulated methylotrophic methanogenesis in laboratory experiments and natural environments (Bose et al., 2008; Chistoserdova, 2011; Chistoserdova et al., 2009; Huang et al., 2018; Singh et al., 2005; Tebbe et al., 2023; Whiticar, 1999; Zhou et al., 2022).

Indirect evidence for the presence of methylated sulfur compounds comes from relatively higher concentrations of $H_2S$, AVS, and CRS at depth (Fig. 2B, 2K), indicating active sulfur cycling despite limited $SO_4^{2-}$ availability. Furthermore, $\delta^{34}S$ values measured in CRS (primarily pyrite) consistently show positive isotopic signatures (7‰ to 10‰) in both the deep eutrophic and middle carbonate zones. While microbial $SO_4^{2-}$ reduction typically produces $^{34}S$-depleted sulfides ($\delta^{34}S < 0$‰) under open-system or moderately sulfate-limited conditions (Bradley et al., 2016; Canfield, 2001; Habicht and Canfield, 1997), the isotopic enrichment observed here is more consistent with either the degradation of sulfurized organic matter or methylated sulfur compounds (Phillips et al., 2022; Raven et al., 2019; Werne et al., 2004). These could simultaneously fuel methylotrophic methanogenesis and pyrite formation. This interpretation warrants confirmation through direct measurements of methylated sulfur species in future studies. Alternatively, the $^{34}S$ enrichment could reflect near complete consumption of a limited $SO_4^{2-}$ pool so that $^{34}S$ sulfide reflects positive values of the original sulfate (Bernasconi et al., 2017)(Fig. 2).

It is important to note that methylotroph distributions could also be influenced by competition for $H_2$ with $CO_2$-reducing hydrogenotrophs. In sulfate-poor anoxic sediments, $H_2$ is typically buffered at low steady-state levels by continuous fermentative supply and rapid consumption—reflecting thermodynamic control rather than chronic scarcity (Conrad, 1999; Schütz et al., 1988; Kessler et al., 2019). Obligately methyl-reducing methanogens have very low $H_2$ thresholds and are predicted to outcompete hydrogenotrophs for $H_2$ when methyl groups are available. Thus, their activity is primarily considered to be limited by the availability of methylated substrates (Borrel et al., 2023; Bueno De Mesquita et al., 2023; Feldewert et al., 2020; Söllinger and Urich, 2019; Speth and Orphan, 2018). Given the dominance of *Methanomassiliicoccales* at depth, we infer that methylated-substrate supply rather than $H_2$ limitation is the primary methanogenic community structuring factor in the deep eutrophic interval. This interpretation is consistent with isotope patterns, as we have recorded

585 comparatively heavier $\delta^{13}C_{DIC}$ in the deep eutrophic layer and a shift to lighter $\delta^{13}C_{DIC}$ above
586 ~30 cm where the relative abundance of $CO_2$-reducing hydrogenotrophic methanogens
587 increased (Fig. 2F).
588 Methylotrophic methanogenesis is typically a minor pathway in freshwater sediments
589 because methylated substrates are scarce (Borrel et al., 2011; Bueno De Mesquita et al., 2023).
590 However, in the deep eutrophic layer, prolonged algal biomass degradation likely generated a
591 reservoir of recalcitrant methylated compounds (Achtnich et al., 1995; Rissanen et al., 2018),
592 favoring methylotrophic methanogens. In contrast, hydrogenotrophic (using $CO_2$ + $H_2$) and
593 acetoclastic (using acetate) methanogens primarily depend on fresh, labile organic matter,
594 which rapidly becomes limited with burial (Achtnich et al., 1995; Meier et al., 2024; Rissanen
595 et al., 2023; Rissanen et al., 2018). Thus, methylotrophs gain a selective advantage in these
596 older, more refractory sediments. Above ~28.5 cm, concurrent with a shift toward more
597 terrestrial organic matter, methylotrophic methanogens decline and hydrogenotrophs
598 progressively dominate (Fig. 4A). We interpret this pattern as consistent with a reduced supply
599 of methylated substrates typically derived from algal organic matter although these compounds
600 were not directly measured.
601 To further support the interpretation of distinct methanogenic pathways, we analyzed
602 the $\varepsilon_{Corg-CH4}$, reflecting the isotopic discrimination during $CH_4$ formation from $C_{org}$ (Fig. 2O).
603 Methanogenesis discriminates against the heavier $^{13}C$ isotope (Conrad, 2005). In theory, when
604 $CH_4$ is produced from $CO_2$ + $H_2$ (hydrogenotrophy), microbes selectively withdraw $^{12}C$ from
605 the DIC pool, leaving residual DIC relatively $^{13}C$-enriched (less negative $\delta^{13}C_{DIC}$); when
606 methylotrophy dominates, $CH_4$ carbon is drawn from methyl pools and $\delta^{13}C_{DIC}$ is affected less.
607 We observed lower ε values in deeper eutrophic sediments compared to shallower zones.
608 Although interpreting specific metabolic pathways from isotopic fractionation is challenging
609 in mixed microbial communities, the contrast in $\varepsilon_{Corg-CH4}$ (Fig. 2O) indicates distinct $CH_4$-
610 producing processes dominate at different sediment depths.
611 Our results support the view that eutrophication leaves a distinct imprint on methanogen
612 stratification in sediments. In contrast to earlier studies that reported either weak vertical
613 structuring (Meier et al., 2024) or only subtle shifts in methanogen dominance (Rissanen et al.,
614 2023), we found clear zonation with Methanomassiliicoccales prevailing in the deepest
615 eutrophic interval, Methanomicrobiaceae in the carbonate-rich middle section, and
616 Methanobacteriaceae dominating the upper eutrophic sediments. Considered alongside these
617 previous observations in other lakes, our findings question the usefulness of broad
618 generalizations and suggest that methanogen communities are primarily shaped by habitat-

specific conditions—such as lithology, organic-matter quality, and redox context—rather than exhibiting universal hydrogenotroph dominance. By comparison, a pronounced vertical structuring of methane-oxidizing bacteria appears more consistent across systems (Mayr et al., 2020; Rissanen et al., 2018; Van Grinsven et al., 2022).

### *4.3* Aerobic methanotrophs are selected by nutrient availability

Within anoxic lacustrine sediments, $CH_4$ is typically oxidized anaerobically (Borrel et al., 2011; Martinez-Cruz et al., 2018). Interestingly, in the anoxic sediments of Lake Joux, anaerobic methanotrophic archaea are not detectable. Sequences related to *Candidatus Methylomirabilis*—capable of intracellular $O_2$ production to fuel methane monooxygenase activity—occur in notable relative sequence abundances but are confined to 16–23 cm depth within the middle carbonate interval, but are relatively scarce compared to their aerobic counterparts. Namely, gammaproteobacterial MOB 16S rRNA gene sequences recovered from Lake Joux sediments are highly abundant (1- 9%) from 19.5 cm upward, despite prevailing anoxic conditions (Fig. 4, 5). The MOB 16S rRNA gene sequences primarily affiliate with Methylococcales, notably the genera *Crenothrix* and *Methylobacter* (Fig. 5). The dominance of Methylococcales-associated MOB in the methane oxidation zone suggests that these taxa serve as the dominant $CH_4$ sink in these nutrient-replete but anoxic surface sediments (Fig. 2N, Fig. 5). Aerobic (and denitrifying) methanotrophy also fractionates carbon, preferentially consuming $^{12}CH_4$. This enriches residual $CH_4$ in $^{13}C$ and can generate lighter (more $^{12}C$) co-localized DIC depending on mixing and available electron acceptors. The paired heavier $\delta^{13}C$-$CH_4$ and lighter $\delta^{13}C$-DIC in the 7.5–0 cm horizon thus support the occurrence of active methane oxidation.

How these aerobic methanotrophs meet their $O_2$ demand below 0.4 cm—where no $O_2$ could be detected, remains unresolved. Nanomolar $O_2$ cannot be excluded, but diffusive supply from the sediment–water interface to higher sediment depths is implausible. While some Methylococcales respire alternative electron acceptors (e.g., nitrate, Fe(III)) at low $O_2$ levels (Li et al., 2023; Van Grinsven et al., 2020; Yang et al., 2025), methane monooxygenase remains $O_2$-dependent for the oxidation of $CH_4$ to methanol. Three microbial mechanisms could generate microscale $O_2$ at depth within the sediment ("dark $O_2$" ): methanobactin-mediated water splitting (Dershwitz et al., 2021), chlorite ($ClO_2^-$) dismutation by (per)chlorate-respiring bacteria (Xu and Logan, 2003), and nitric-oxide dismutation as described for NC10 bacteria (Ettwig et al., 2010).

Water lysis has been proposed as a potential mechanism for $O_2$ generation via methanobactin-mediated metal reduction, particularly under metal-rich conditions. (Dershwitz et al., 2021). This process has been primarily associated with Alphaproteobacterial methanotrophs, which are not prevalent in Lake Joux. Chlorite dismutation, catalyzed by chlorite dismutase found in over 60 genera across 13 phyla (Barnum and Coates, 2023), could be a source of $O_2$, as Pseudomonadota and Actinobacteria are abundant in these sediments (Fig. 3A). However, environmental levels of (per)chlorate are likely too low to support this pathway at significant levels (Lv et al., 2019; Miller et al., 2014; Wang et al., 2024).

One potential source of *in-situ* $O_2$ is nitric oxide dismutation catalyzed by the nitric oxide dismutase (NOD) enzyme, which has been recently attributed to multiple bacterial lineages, including several families within the phylum Bacteroidota (Ruff et al., 2024). In Lake Joux, putatively NOD-containing Bacteroidota account for ~0.54 ± 0.2% of the microbial community in the upper eutrophic sediments, suggesting this pathway may contribute to localized $O_2$ production. However, as NOD is not encoded by all representatives of these taxa, we can not perform further reliable abundance estimates of NOD based on the available 16S rRNA gene amplicon data. The mechanism of $O_2$ production is nevertheless consistent with our geochemical context: porewater $NO_2^-$ remained near detection limit with no subsurface maximum (Fig. S2), indicating rapid NO*x* turnover typical of energy-limited sediments. Independent work shows some gammaproteobacterial methanotrophs, including *Crenothrix* and *Methylobacter*, possess genes for respiratory $NO_3^-$ reduction (Almog et al., 2024; He et al., 2022; Martinez-Cruz et al., 2017; Milucka et al., 2012; Schorn et al., 2024). Active $NO_3^-$ respiration has only been demonstrated experimentally for *Methylomonas denitrificans* cultures (Kits et al., 2015) and indirectly by denitrification gene expression by MOB in Lake Zug (Schorn et al., 2024). The latter study revealed that *Crenothrix* and *Methylobacter* related microorganisms continue $CH_4$ oxidation in hypoxic and anoxic regions of the water column by performing denitrification or fermentation-based methanotrophy (Schorn et al., 2024). In Lake Joux, these same MOB taxa dominate the highly reducing, upper eutrophic sediments (Fig. 4B).

The positive covariance of *Crenothrix* and *Methylobacter* with $NO_3^-$ and $PO_4^{3-}$ is also consistent with nutrient-stimulated MOB activity and/or a shared response to favorable near-surface conditions. While the source of surprisingly high $NO_3^-$ concentrations cannot be resolved here, possible mechanisms of $NO_3^-$ generation include oxidation of $NH_4^+$ by Mn(IV) or Fe(III) oxides. Importantly, the MOB–nutrient correlations may also reflect a shared response to favorable near-surface conditions (e.g., sustained inputs of labile organic matter or

higher porosity), rather than direct nutrient control. Nevertheless, it has been experimentally demonstrated that $PO_4^{3-}$, $NO_3^-$, and $NH_4^+$ additions can directly enhance $CH_4$ oxidation rates by MOB and, in particular, *Methylobacter* (Almog et al., 2024; Kits et al., 2015; Nijman et al., 2022; Xia et al., 2021; Yang et al., 2025). Taken together, these observations suggest that nutrient availability may play a direct role in shaping the structure and activity of MOB communities.

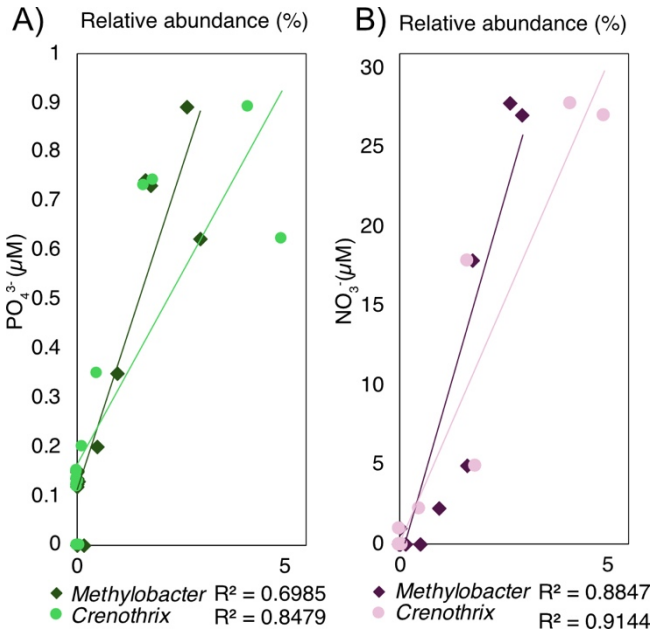


**Figure 5** - (A) Correlation between $PO_4^{3-}$ concentration and the relative sequence abundance of *Crenothrix* and *Methylobacter*. (B) Correlation between $NO_3^-$ concentration and the relative sequence abundance of *Crenothrix* and *Methylobacter*.

## 5. Conclusion

Our results show that historical eutrophication left a lasting sedimentary legacy that structures contemporary methane-cycling microbial communities, selecting methylotrophic methanogens. In upper eutrophic, anoxic sediments, the surprisingly high relative sequence abundances of MOB (up to ~9%) specifically Methylococcales-affiliated Gammaproteobacteria, co-vary with elevated $NO_3^-$ and $PO_4^{3-}$ concentrations. This suggests that eutrophication can simultaneously stimulate $CH_4$ production and enhance its oxidation by shaping microbial assemblages.

As eutrophication continues to alter freshwater systems globally, understanding nutrient- and substrate-driven shifts in $CH_4$-cycling communities becomes increasingly important. Future studies should focus on elucidating the in situ activity of aerobic methanotrophs and molecular mechanism of methane oxidation under anoxic conditions, as

presumably aerobic MOB have been widely reported in anoxic sediments (Almog et al., 2024; Ruff et al., 2024; Schorn et al., 2024). Combining molecular, isotopic, and geochemical approaches will be essential to better constrain methane fluxes in lakes undergoing or recovering from eutrophication.

## Data availability

All geochemical data are included in this published article and its supplementary information files. The 16S rRNA gene amplicon sequencing data has been deposited at the Sequence Read Archive under the BioProject accession PRJNA1207472.

## Author contribution

ABS contributed to conceptualization, data curation, formal analysis, funding acquisition, methodology, supervision, validation, visualization, writing original draft preparation, review, and editing. ERBB contributed to data curation, formal analysis, and manuscript editing; SK contributed to data curation, formal analysis, and manuscript editing; MEM contributed to resources and manuscript editing; JS contributed to data curation, formal analysis, methodology, validation, visualization, designing and implementing computer codes, and writing original draft preparation, review, and editing. PP contributed to conceptualization, formal analysis, funding acquisition, supervision, validation, visualization, writing original draft preparation, review, and editing. JSB contributed to conceptualization, formal analysis, funding acquisition, supervision, validation, visualization, writing original draft preparation, review, and editing.

## Competing interests

The authors declare that they have no conflict of interest.

## Acknowledgments

The authors would like to extend their gratitude to Floreana Marie Miesen (UNIL) for her invaluable support with fieldwork and logistics; to Dr. Carsten Schubert (EAWAG) for providing access to laboratory facilities for methane analyses; to Dr. Giulia Ceriotti (UNIL) for analytical and logistical support with methane analyses; to Laetitia Monbaron and Micaela Faria (UNIL) for their technical assistance in the laboratory; to Jorge Spangenberg (UNIL) for his support in methodology development and analytical assistance; to Frédéric Lardet for

assistance with Fig. 1; and to Dr. William Leavitt (The University of Utah) for his help during fieldwork. Special thanks are also due to the Fondation Agassiz for the individual grant awarded to the first author, ABS, which made this study possible. The amplicon sequencing section of this work has been achieved using the Life Science Compute Cluster (LiSC) of the University of Vienna.

## Financial Support

This study was funded by the 2022 Fondation Agassiz awarded to ABS.

## References

Achtnich, C., Bak, F., and Conrad, R.: Competition for electron donors among nitrate reducers, ferric iron reducers, sulfate reducers, and methanogens in anoxic paddy soil, Biology and fertility of soils, 19, 65-72, 1995.

Almog, G., Rubin-Blum, M., Murrell, J. C., Vigderovich, H., Eckert, W., Larke-Mejía, N., and Sivan, O.: Survival strategies of aerobic methanotrophs to hypoxia in methanogenic lake sediments, 2024.

Apprill, A., McNally, S., Parsons, R., and Weber, L.: Minor revision to V4 region SSU rRNA 806R gene primer greatly increases detection of SAR11 bacterioplankton, Aquatic Microbial Ecology, 75, 129-137, 2015.

Barnett, D. J., Arts, I. C., and Penders, J.: microViz: an R package for microbiome data visualization and statistics, Journal of Open Source Software, 6, 3201, 2021.

Barnum, T. P. and Coates, J. D.: Chlorine redox chemistry is widespread in microbiology, The ISME journal, 17, 70-83, 2023.

Bastviken, D., Cole, J., Pace, M., and Tranvik, L.: Methane emissions from lakes: Dependence of lake characteristics, two regional assessments, and a global estimate, Global biogeochemical cycles, 18, 2004.

Bastviken, D., Cole, J. J., Pace, M. L., and Van de Bogert, M. C.: Fates of methane from different lake habitats: Connecting whole-lake budgets and $CH_4$ emissions, Journal of Geophysical Research: Biogeosciences, 113, 2008.

Bastviken, D., Tranvik, L. J., Downing, J. A., Crill, P. M., and Enrich-Prast, A.: Freshwater methane emissions offset the continental carbon sink, Science, 331, 50-50, 2011.

Beaulieu, J. J., DelSontro, T., and Downing, J. A.: Eutrophication will increase methane emissions from lakes and impoundments during the 21$^{st}$ century, Nature communications, 10, 1375, 2019.

Bernasconi, S. M., Meier, I., Wohlwend, S., Brack, P., Hochuli, P. A., Bläsi, H., Wortmann, U. G., and Ramseyer, K.: An evaporite-based high-resolution sulfur isotope record of Late Permian and Triassic seawater sulfate, Geochimica et Cosmochimica Acta, 204, 331-349, 2017.

Borrel, G., Jézéquel, D., Biderre-Petit, C., Morel-Desrosiers, N., Morel, J.-P., Peyret, P., Fonty, G., and Lehours, A.-C.: Production and consumption of methane in freshwater lake ecosystems, Research in microbiology, 162, 832-847, 2011.

Borrel, G., Fadhlaoui, K., Ben Hania, W., Gaci, N., Pehau-Arnaudet, G., Chaudhary, P. P., Vandekerckove, P., Ballet, N., Alric, M., and O'toole, P. W.: Methanomethylophilus alvi gen. nov., sp. nov., a Novel Hydrogenotrophic Methyl-Reducing Methanogenic Archaea of the

Order Methanomassiliicoccales Isolated from the Human Gut and Proposal of the Novel Family Methanomethylophilaceae fam. nov, Microorganisms, 11, 2794, 2023.
Bose, A., Pritchett, M. A., and Metcalf, W. W.: Genetic analysis of the methanol-and methylamine-specific methyltransferase 2 genes of Methanosarcina acetivorans C2A, Journal of bacteriology, 190, 4017-4026, 2008.
Bradley, A., Leavitt, W., Schmidt, M., Knoll, A. H., Girguis, P. R., and Johnston, D. T.: Patterns of sulfur isotope fractionation during microbial sulfate reduction, Geobiology, 14, 91-101, 2016.
Brick, S., Niggemann, J., Reckhardt, A., Könneke, M., and Engelen, B.: Interstitial microbial communities of coastal sediments are dominated by Nanoarchaeota, Frontiers in Microbiology, 16, 1532193, 2025.
Bueno de Mesquita, C. P., Wu, D., and Tringe, S. G.: Methyl-based methanogenesis: an ecological and genomic review, Microbiology and Molecular Biology Reviews, 87, e00024-00022, 2023.
Callahan, B. J., Sankaran, K., Fukuyama, J. A., McMurdie, P. J., and Holmes, S. P.: Bioconductor workflow for microbiome data analysis: from raw reads to community analyses, F1000Research, 5, 2016a.
Callahan, B. J., McMurdie, P. J., Rosen, M. J., Han, A. W., Johnson, A. J. A., and Holmes, S. P.: DADA2: High-resolution sample inference from Illumina amplicon data, Nature methods, 13, 581-583, 2016b.
Canfield, D. E.: Isotope fractionation by natural populations of sulfate-reducing bacteria, Geochimica et Cosmochimica Acta, 65, 1117-1124, 2001.
Chen, M., Conroy, J. L., Sanford, R. A., Wyman-Feravich, D. A., Chee-Sanford, J. C., and Connor, L. M.: Tropical lacustrine sediment microbial community response to an extreme El Niño event, Scientific reports, 13, 6868, 2023.
Chistoserdova, L.: Modularity of methylotrophy, revisited, Environmental microbiology, 13, 2603-2622, 2011.
Chistoserdova, L., Kalyuzhnaya, M. G., and Lidstrom, M. E.: The expanding world of methylotrophic metabolism, Annual review of microbiology, 63, 477-499, 2009.
Cline, J. D.: Spectrophotometric determination of hydrogen sulfide in natural waters, Limnology and Oceanography, 14, 454-458, 1969.
Conrad, R.: Contribution of hydrogen to methane production and control of hydrogen concentrations in methanogenic soils and sediments, FEMS microbiology Ecology, 28, 193-202, 1999.
Conrad, R.: Quantification of methanogenic pathways using stable carbon isotopic signatures: a review and a proposal, Organic geochemistry, 36, 739-752, 2005.
Conrad, R.: Importance of hydrogenotrophic, acetoclastic and methylotrophic methanogenesis for methane production in terrestrial, aquatic and other anoxic environments: a mini review, Pedosphere, 30, 25-39, 2020.
Dean, J. F., Middelburg, J. J., Röckmann, T., Aerts, R., Blauw, L. G., Egger, M., Jetten, M. S., de Jong, A. E., Meisel, O. H., and Rasigraf, O.: Methane feedbacks to the global climate system in a warmer world, Reviews of Geophysics, 56, 207-250, 2018.
Dershwitz, P., Bandow, N. L., Yang, J., Semrau, J. D., McEllistrem, M. T., Heinze, R. A., Fonseca, M., Ledesma, J. C., Jennett, J. R., and DiSpirito, A. M.: Oxygen generation via water splitting by a novel biogenic metal ion-binding compound, Applied and Environmental Microbiology, 87, e00286-00221, 2021.
Deutzmann, J. S. and Schink, B.: Anaerobic oxidation of methane in sediments of Lake Constance, an oligotrophic freshwater lake, Applied and environmental microbiology, 77, 4429-4436, 2011.
Dubois, N.: Traces of history in the sediments of Lake Joux, 2016.

Ellenbogen, J. B., Borton, M. A., McGivern, B. B., Cronin, D. R., Hoyt, D. W., Freire-Zapata, V., McCalley, C. K., Varner, R. K., Crill, P. M., and Wehr, R. A.: Methylotrophy in the Mire: direct and indirect routes for methane production in thawing permafrost, Msystems, 9, e00698-00623, 2024.
Ettwig, K. F., Butler, M. K., Le Paslier, D., Pelletier, E., Mangenot, S., Kuypers, M. M., Schreiber, F., Dutilh, B. E., Zedelius, J., and de Beer, D.: Nitrite-driven anaerobic methane oxidation by oxygenic bacteria, Nature, 464, 543-548, 2010.
Feldewert, C., Lang, K., and Brune, A.: The hydrogen threshold of obligately methyl-reducing methanogens, FEMS Microbiology Letters, 367, fnaa137, 2020.
Fiskal, A., Deng, L., Michel, A., Eickenbusch, P., Han, X., Lagostina, L., Zhu, R., Sander, M., Schroth, M. H., and Bernasconi, S. M.: Effects of eutrophication on sedimentary organic carbon cycling in five temperate lakes, Biogeosciences, 16, 3725-3746, 2019.
Garcia, J.-L., Patel, B. K., and Ollivier, B.: Taxonomic, phylogenetic, and ecological diversity of methanogenic Archaea, Anaerobe, 6, 205-226, 2000.
Habicht, K. S. and Canfield, D. E.: Sulfur isotope fractionation during bacterial sulfate reduction in organic-rich sediments, Geochimica et Cosmochimica Acta, 61, 5351-5361, 1997.
Han, X.: Influence of eutrophication on microbial community structure, organic carbon sources, and organic carbon degradation in lake sediments through time, ETH Zurich, 2020.
Hanson, R. S. and Hanson, T. E.: Methanotrophic bacteria, Microbiological reviews, 60, 439-471, 1996.
He, R., Wang, J., Pohlman, J. W., Jia, Z., Chu, Y.-X., Wooller, M. J., and Leigh, M. B.: Metabolic flexibility of aerobic methanotrophs under anoxic conditions in Arctic lake sediments, The ISME Journal, 16, 78-90, 2022.
Ho, A., Kerckhof, F. M., Luke, C., Reim, A., Krause, S., Boon, N., and Bodelier, P. L.: Conceptualizing functional traits and ecological characteristics of methane-oxidizing bacteria as life strategies, Environmental Microbiology Reports, 5, 335-345, 2013.
Holmer, M. and Storkholm, P.: Sulphate reduction and sulphur cycling in lake sediments: a review, Freshwater Biology, 46, 431-451, 2001.
Hoops, S. L. and Knights, D.: LMdist: Local Manifold distance accurately measures beta diversity in ecological gradients, Bioinformatics, 39, btad727, 2023.
Huang, H., Xu, X., Shi, C., Liu, X., and Wang, G.: Response of taste and odor compounds to elevated cyanobacteria biomass and temperature, Bulletin of environmental contamination and toxicology, 101, 272-278, 2018.
Huang, R., Soneson, C., Ernst, F. G., Rue-Albrecht, K. C., Yu, G., Hicks, S. C., and Robinson, M. D.: TreeSummarizedExperiment: a S4 class for data with hierarchical structure, F1000Research, 9, 1246, 2021.
Jarett, J. K., Nayfach, S., Podar, M., Inskeep, W., Ivanova, N. N., Munson-McGee, J., Schulz, F., Young, M., Jay, Z. J., and Beam, J. P.: Single-cell genomics of co-sorted Nanoarchaeota suggests novel putative host associations and diversification of proteins involved in symbiosis, Microbiome, 6, 1-14, 2018.
Jørgensen, B. B., Weber, A., and Zopfi, J.: Sulfate reduction and anaerobic methane oxidation in Black Sea sediments, Deep Sea Research Part I: Oceanographic Research Papers, 48, 2097-2120, 2001.
Kessler, A. J., Chen, Y.-J., Waite, D. W., Hutchinson, T., Koh, S., Popa, M. E., Beardall, J., Hugenholtz, P., Cook, P. L., and Greening, C.: Bacterial fermentation and respiration processes are uncoupled in anoxic permeable sediments, Nature microbiology, 4, 1014-1023, 2019.
Khatun, S., Berg, J. S., Jézéquel, D., Moiron, M., Escoffier, N., Schubert, C. J., Bouffard, D., and Perga, M. E.: Long-range transport of littoral methane explains the metalimnetic methane peak in a large lake, Limnology and Oceanography, 69, 2095-2108, 2024.

Kits, K. D., Klotz, M. G., and Stein, L. Y.: Methane oxidation coupled to nitrate reduction under hypoxia by the Gammaproteobacterium *Methylomonas denitrificans, sp.* nov. type strain FJG1, Environmental microbiology, 17, 3219-3232, 2015.
Knief, C.: Diversity and habitat preferences of cultivated and uncultivated aerobic methanotrophic bacteria evaluated based on *pmoA* as molecular marker, Frontiers in microbiology, 6, 1346, 2015.
Knittel, K. and Boetius, A.: Anaerobic oxidation of methane: progress with an unknown process, Annual review of microbiology, 63, 311-334, 2009.
Lamb, A. L., Wilson, G. P., and Leng, M. J.: A review of coastal palaeoclimate and relative sea-level reconstructions using δ13C and C/N ratios in organic material, Earth-Science Reviews, 75, 29-57, 2006.
Lavrieux, M., Schubert, C. J., Hofstetter, T., Eglinton, T. I., Hajdas, I., Wacker, L., and Dubois, N.: From medieval land clearing to industrial development: 800 years of human-impact history in the Joux Valley (Swiss Jura), The Holocene, 27, 1443-1454, 2017.
Li, B., Tao, Y., Mao, Z., Gu, Q., Han, Y., Hu, B., Wang, H., Lai, A., Xing, P., and Wu, Q. L.: Iron oxides act as an alternative electron acceptor for aerobic methanotrophs in anoxic lake sediments, Water Research, 234, 119833, 2023.
Lods-Crozet, B., Reymond, O., and Strawczynski, A.: Evaluation de la qualité chimique et biologique du lac de Joux (Jura Suisse) entre 1985 et 2004, Bull Soc Ne Sci Nat, 129, 29-47, 2006.
Lv, P.-L., Shi, L.-D., Wang, Z., Rittmann, B., and Zhao, H.-P.: Methane oxidation coupled to perchlorate reduction in a membrane biofilm batch reactor, Science of the Total Environment, 667, 9-15, 2019.
Magny, M., Gauthier, E., Vannière, B., and Peyron, O.: Palaeohydrological changes and human-impact history over the last millennium recorded at Lake Joux in the Jura Mountains, Switzerland, The Holocene, 18, 255-265, 2008.
Martinez-Cruz, K., Sepulveda-Jauregui, A., Casper, P., Anthony, K. W., Smemo, K. A., and Thalasso, F.: Ubiquitous and significant anaerobic oxidation of methane in freshwater lake sediments, Water Research, 144, 332-340, 2018.
Martinez-Cruz, K., Leewis, M.-C., Herriott, I. C., Sepulveda-Jauregui, A., Anthony, K. W., Thalasso, F., and Leigh, M. B.: Anaerobic oxidation of methane by aerobic methanotrophs in sub-Arctic lake sediments, Science of the Total Environment, 607, 23-31, 2017.
Mayr, M. J., Zimmermann, M., Guggenheim, C., Brand, A., and Bürgmann, H.: Niche partitioning of methane-oxidizing bacteria along the oxygen–methane counter gradient of stratified lakes, The ISME journal, 14, 274-287, 2020.
McLaren, M. R. and Callahan, B. J.: Silva 138.1 prokaryotic SSU taxonomic training data formatted for DADA2, Zenodo, 2021.
McMurdie, P. J. and Holmes, S.: phyloseq: an R package for reproducible interactive analysis and graphics of microbiome census data, PloS one, 8, e61217, 2013.
Meier, D., van Grinsven, S., Michel, A., Eickenbusch, P., Glombitza, C., Han, X., Fiskal, A., Bernasconi, S., Schubert, C. J., and Lever, M. A.: Hydrogen-independent $CO_2$ reduction dominates methanogenesis in five temperate lakes that differ in trophic states, ISME Communications, ycae089, 2024.
Meyers, P. A.: Preservation of elemental and isotopic source identification of sedimentary organic matter, Chemical geology, 114, 289-302, 1994.
Miller, L. G., Baesman, S. M., Carlström, C. I., Coates, J. D., and Oremland, R. S.: Methane oxidation linked to chlorite dismutation, Frontiers in Microbiology, 5, 275, 2014.
Milucka, J., Ferdelman, T. G., Polerecky, L., Franzke, D., Wegener, G., Schmid, M., Lieberwirth, I., Wagner, M., Widdel, F., and Kuypers, M. M.: Zero-valent sulphur is a key intermediate in marine methane oxidation, Nature, 491, 541-546, 2012.

Mitchell, E., van der Knaap, W. O., van Leeuwen, J. F., Buttler, A., Warner, B. G., and Gobat, J.-M.: The palaeoecological history of the Praz-Rodet bog (Swiss Jura) based on pollen, plant macrofossils and testate amoebae (Protozoa), The Holocene, 11, 65-80, 2001.
Monchamp, M.-È., Bruel, R., Frossard, V., McGowan, S., Lavrieux, M., Muschick, M., Perga, M.-É., and Dubois, N.: Paleoecological evidence for a multi-trophic regime shift in a perialpine lake (Lake Joux, Switzerland), Anthropocene, 35, 100301, 2021.
Morales-Williams, A. M., Wanamaker Jr, A. D., and Downing, J. A.: Cyanobacterial carbon concentrating mechanisms facilitate sustained CO 2 depletion in eutrophic lakes, Biogeosciences, 14, 2865-2875, 2017.
Nijman, T. P., Amado, A. M., Bodelier, P. L., and Veraart, A. J.: Relief of phosphate limitation stimulates methane oxidation, Frontiers in Environmental Science, 10, 804512, 2022.
Oswald, K., Milucka, J., Brand, A., Hach, P., Littmann, S., Wehrli, B., Kuypers, M. M., and Schubert, C. J.: Aerobic gammaproteobacterial methanotrophs mitigate methane emissions from oxic and anoxic lake waters, Limnology and Oceanography, 61, S101-S118, 2016.
Parada, A. E., Needham, D. M., and Fuhrman, J. A.: Every base matters: assessing small subunit rRNA primers for marine microbiomes with mock communities, time series and global field samples, Environmental microbiology, 18, 1403-1414, 2016.
Penger, J., Conrad, R., and Blaser, M.: Stable carbon isotope fractionation by methylotrophic methanogenic archaea, Applied and environmental microbiology, 78, 7596-7602, 2012.
Phillips, A. A., White, M. E., Seidel, M., Wu, F., Pavia, F. F., Kemeny, P. C., Ma, A. C., Aluwihare, L. I., Dittmar, T., and Sessions, A. L.: Novel sulfur isotope analyses constrain sulfurized porewater fluxes as a minor component of marine dissolved organic matter, Proceedings of the National Academy of Sciences, 119, e2209152119, 2022.
Piguet, A.: Le territoire et la commune du Lieu jusqu'en 1536, 1946.
Pjevac, P., Hausmann, B., Schwarz, J., Kohl, G., Herbold, C. W., Loy, A., and Berry, D.: An economical and flexible dual barcoding, two-step PCR approach for highly multiplexed amplicon sequencing, Frontiers in microbiology, 12, 669776, 2021.
Quast, C., Pruesse, E., Yilmaz, P., Gerken, J., Schweer, T., Yarza, P., Peplies, J., and Glöckner, F. O.: The SILVA ribosomal RNA gene database project: improved data processing and web-based tools, Nucleic acids research, 41, D590-D596, 2012.
Raven, M., Fike, D., Gomes, M., and Webb, S.: Chemical and isotopic evidence for organic matter sulfurization in redox gradients around mangrove roots, Frontiers in Earth Science, 7, 98, 2019.
Reis, P. C., Thottathil, S. D., Ruiz-González, C., and Prairie, Y. T.: Niche separation within aerobic methanotrophic bacteria across lakes and its link to methane oxidation rates, Environmental microbiology, 22, 738-751, 2020.
Reis, P. C., Tsuji, J. M., Weiblen, C., Schiff, S. L., Scott, M., Stein, L. Y., and Neufeld, J. D.: Enigmatic persistence of aerobic methanotrophs in oxygen-limiting freshwater habitats, The ISME Journal, 18, wrae041, 2024.
Rissanen, A. J., Saarenheimo, J., Tiirola, M., Peura, S., Aalto, S. L., Karvinen, A., and Nykänen, H.: Gammaproteobacterial methanotrophs dominate methanotrophy in aerobic and anaerobic layers of boreal lake waters, Aquatic Microbial Ecology, 81, 257-276, 2018.
Rissanen, A. J., Jilbert, T., Simojoki, A., Mangayil, R., Aalto, S. L., Khanongnuch, R., Peura, S., and Jäntti, H.: Organic matter lability modifies the vertical structure of methane-related microbial communities in lake sediments, Microbiology spectrum, 11, e01955-01923, 2023.
Ruff, S. E., Schwab, L., Vidal, E., Hemingway, J. D., Kraft, B., and Murali, R.: Widespread occurrence of dissolved oxygen anomalies, aerobic microbes, and oxygen-producing metabolic pathways in apparently anoxic environments, FEMS Microbiology Ecology, 100, fiae132, 2024.

Sanches, L. F., Guenet, B., Marinho, C. C., Barros, N., and de Assis Esteves, F.: Global regulation of methane emission from natural lakes, Scientific Reports, 9, 255, 2019.
Saunois, M., Stavert, A., Poulter, B., Bousquet, P., Canadell, J., Jackson, R., Raymond, P., Dlugokencky, E., Houweling, S., and Patra, P.: The Global Methane Budget 2000–2017, Earth Syst. Sci. Data, 12, 1561–1623, 2020.
Schorn, S., Graf, J. S., Littmann, S., Hach, P. F., Lavik, G., Speth, D. R., Schubert, C. J., Kuypers, M. M., and Milucka, J.: Persistent activity of aerobic methane-oxidizing bacteria in anoxic lake waters due to metabolic versatility, Nature Communications, 15, 5293, 2024.
Schütz, H., Conrad, R., Goodwin, S., and Seiler, W.: Emission of hydrogen from deep and shallow freshwater environments, Biogeochemistry, 5, 295-311, 1988.
Singh, N., Kendall, M. M., Liu, Y., and Boone, D. R.: Isolation and characterization of methylotrophic methanogens from anoxic marine sediments in Skan Bay, Alaska: description of Methanococcoides alaskense sp. nov., and emended description of Methanosarcina baltica, International journal of systematic and evolutionary microbiology, 55, 2531-2538, 2005.
Söllinger, A. and Urich, T.: Methylotrophic methanogens everywhere—physiology and ecology of novel players in global methane cycling, Biochemical Society Transactions, 47, 1895-1907, 2019.
Spangenberg, J. E. and Bosco-Santos, A.: Sulfur isotope analyses using 3× elemental analysis/isotope ratio mass spectrometry: Saving helium and energy while reducing analytical time and costs, Rapid Communications in Mass Spectrometry, 38, e9866, 2024.
Speth, D. R. and Orphan, V. J.: Metabolic marker gene mining provides insight in global mcrA diversity and, coupled with targeted genome reconstruction, sheds further light on metabolic potential of the Methanomassiliicoccales, PeerJ, 6, e5614, 2018.
Sun, J., Mausz, M. A., Chen, Y., and Giovannoni, S. J.: Microbial trimethylamine metabolism in marine environments, Environmental Microbiology, 21, 513-520, 2019.
Tamas, I., Smirnova, A. V., He, Z., and Dunfield, P. F.: The (d) evolution of methanotrophy in the Beijerinckiaceae—a comparative genomics analysis, The ISME journal, 8, 369-382, 2014.
Tebbe, D. A., Gruender, C., Dlugosch, L., Lõhmus, K., Rolfes, S., Könneke, M., Chen, Y., Engelen, B., and Schäfer, H.: Microbial drivers of DMSO reduction and DMS-dependent methanogenesis in saltmarsh sediments, The ISME Journal, 17, 2340-2351, 2023.
Tranvik, L. J., Downing, J. A., Cotner, J. B., Loiselle, S. A., Striegl, R. G., Ballatore, T. J., Dillon, P., Finlay, K., Fortino, K., and Knoll, L. B.: Lakes and reservoirs as regulators of carbon cycling and climate, Limnology and oceanography, 54, 2298-2314, 2009.
Tsola, S. L., Zhu, Y., Ghurnee, O., Economou, C. K., Trimmer, M., and Eyice, Ö.: Diversity of dimethylsulfide-degrading methanogens and sulfate-reducing bacteria in anoxic sediments along the Medway Estuary, UK, Environmental Microbiology, 23, 4434-4449, 2021.
van Grinsven, S., Meier, D. V., Michel, A., Han, X., Schubert, C. J., and Lever, M. A.: Redox zone and trophic state as drivers of methane-oxidizing bacterial abundance and community structure in lake sediments, Frontiers in Environmental Science, 10, 857358, 2022.
van Grinsven, S., Sinninghe Damsté, J. S., Abdala Asbun, A., Engelmann, J. C., Harrison, J., and Villanueva, L.: Methane oxidation in anoxic lake water stimulated by nitrate and sulfate addition, Environmental microbiology, 22, 766-782, 2020.
Vekeman, B., Kerckhof, F. M., Cremers, G., De Vos, P., Vandamme, P., Boon, N., Op den Camp, H. J., and Heylen, K.: New Methyloceanibacter diversity from North Sea sediments includes methanotroph containing solely the soluble methane monooxygenase, Environmental microbiology, 18, 4523-4536, 2016.
Veraart, A. J., Steenbergh, A. K., Ho, A., Kim, S. Y., and Bodelier, P. L.: Beyond nitrogen: the importance of phosphorus for $CH_4$ oxidation in soils and sediments, Geoderma, 259, 337-346, 2015.

Wang, X.-C. and Lee, C.: Sources and distribution of aliphatic amines in salt marsh sediment, Organic Geochemistry, 22, 1005-1021, 1994.
Wang, Y., Liu, X., Wu, M., and Guo, J.: Methane-Driven Perchlorate Reduction by a Microbial Consortium, Environmental Science & Technology, 58, 13370-13379, 2024.
Wegener, G. and Boetius, A.: An experimental study on short-term changes in the anaerobic oxidation of methane in response to varying methane and sulfate fluxes, Biogeosciences, 6, 867-876, 2009.
Wegener, G., Krukenberg, V., Riedel, D., Tegetmeyer, H. E., and Boetius, A.: Intercellular wiring enables electron transfer between methanotrophic archaea and bacteria, Nature, 526, 587-590, 2015.
Wei, H., Wang, M., Ya, M., and Xu, C.: The denitrifying anaerobic methane oxidation process and microorganisms in the environments: a review, Frontiers in Marine Science, 9, 1038400, 2022.
Wei, T.: i Simko V.(2021). R package'corrplot': Visualization of a Correlation Matrix.(Version 0.92), Available at< Available at https://github. com/taiyun/corrplot>. Accessed on March, 20, 2024.
Werne, J. P., Hollander, D. J., Lyons, T. W., and Damsté, J. S. S.: Organic sulfur biogeochemistry: recent advances and future research directions, 2004.
Whiticar, M. J.: Carbon and hydrogen isotope systematics of bacterial formation and oxidation of methane, Chemical Geology, 161, 291-314, 1999.
Xia, F., Jiang, Q.-Y., Zhu, T., Zou, B., Liu, H., and Quan, Z.-X.: Ammonium promoting methane oxidation by stimulating the Type Ia methane-oxidizing bacteria in tidal flat sediments of the Yangtze River estuary, Science of the Total Environment, 793, 148470, 2021.
Xie, Z., Li, W., Yang, K., Wang, X., Xiong, S., and Zhang, X.: Bacterial and Archaeal Communities in Erhai Lake Sediments: Abundance and Metabolic Insight into a Plateau Lake at the Edge of Eutrophication, Microorganisms, 12, 1617, 2024.
Xu, J. and Logan, B. E.: Measurement of chlorite dismutase activities in perchlorate respiring bacteria, Journal of microbiological methods, 54, 239-247, 2003.
Yan, X., Xu, X., Wang, M., Wang, G., Wu, S., Li, Z., Sun, H., Shi, A., and Yang, Y.: Climate warming and cyanobacteria blooms: Looks at their relationships from a new perspective, Water Research, 125, 449-457, 2017.
Yang, R., Peng, C., Mo, Y., Kleindienst, S., Li, S., Wang, J., Kappler, A., Wang, Z., and Lu, L.: Electron acceptors modulate methane oxidation and active methanotrophic communities in anoxic urban wetland sediments, Applied and Environmental Microbiology, 91, e00386-00325, 2025.
Yang, Y., Chen, J., Tong, T., Xie, S., and Liu, Y.: Influences of eutrophication on methanogenesis pathways and methanogenic microbial community structures in freshwater lakes, Environmental Pollution, 260, 114106, 2020.
Yang, Y., Chen, J., Chen, X., Jiang, Q., Liu, Y., and Xie, S.: Cyanobacterial bloom induces structural and functional succession of microbial communities in eutrophic lake sediments, Environmental Pollution, 284, 117157, 2021.
Yang, Y., Chen, J., Tong, T., Li, B., He, T., Liu, Y., and Xie, S.: Eutrophication influences methanotrophic activity, abundance and community structure in freshwater lakes, Science of the Total Environment, 662, 863-872, 2019.
Yvon-Durocher, G., Allen, A. P., Bastviken, D., Conrad, R., Gudasz, C., St-Pierre, A., Thanh-Duc, N., and Del Giorgio, P. A.: Methane fluxes show consistent temperature dependence across microbial to ecosystem scales, Nature, 507, 488-491, 2014.
Zhao, Y., Liu, Y., Cao, S., Hao, Q., Liu, C., and Li, Y.: Anaerobic oxidation of methane driven by different electron acceptors: A review, Science of The Total Environment, 174287, 2024.

Zhou, C., Peng, Y., Yu, M., Deng, Y., Chen, L., Zhang, L., Xu, X., Zhang, S., Yan, Y., and Wang, G.: Severe cyanobacteria accumulation potentially induces methylotrophic methane producing pathway in eutrophic lakes, Environmental Pollution, 292, 118443, 2022.
Zhu, Y., Chen, X., Yang, Y., and Xie, S.: Impacts of cyanobacterial biomass and nitrate nitrogen on methanogens in eutrophic lakes, Science of The Total Environment, 848, 157570, 2022.